

Friction between solids

BY JUDITH A. HARRISON^{1,*}, GUANGTU GAO¹, J. DAVID SCHALL¹,
M. TODD KNIPPENBERG¹ AND PAUL T. MIKULSKI²

¹*Department of Chemistry, and* ²*Department of Physics,*
United States Naval Academy, Annapolis, MD 21402, USA

The theoretical examination of the friction between solids is discussed with a focus on self-assembled monolayers, carbon-containing materials and antiwear additives. Important findings are illustrated by describing examples where simulations have complemented experimental work by providing a deeper understanding of the molecular origins of friction. Most of the work discussed herein makes use of classical molecular dynamics (MD) simulations. Of course, classical MD is not the only theoretical tool available to study friction. In view of that, a brief review of the early models of friction is also given. It should be noted that some topics related to the friction between solids, i.e. theory of electronic friction, are not discussed here but will be discussed in a subsequent review.

Keywords: atomic-scale friction; molecular dynamics; diamond; tribochemistry; SAMS; adhesion

1. Introduction

The field of tribology is one of the oldest, dating back to the construction of the Egyptian pyramids. The modern study of tribology began with Leonardo da Vinci (1452–1519) when he deduced the laws governing the motion of a rectangular block sliding over a planar surface (Dowson 1998; Krim 2002). Since da Vinci's work was unpublished, these observations were rediscovered by Amontons in 1699. His two basic laws of friction are: (i) friction force is proportional to the normal load and (ii) the friction force is independent of the contact area. In 1781, Coulomb verified these observations and determined that the friction force is independent of velocity for ordinary sliding speeds.

Despite the fact that these friction laws hold for a variety of macroscopic systems, they have defied attempts to explain them on a fundamental (or microscopic) level (Krim 2002). The advent of new experimental techniques to examine the fundamental aspects of friction has renewed interest in the field of tribology in the last few decades. One of the first experimental techniques to be developed for the fundamental studies of friction was the surface force apparatus (SFA; Ruths & Israelachvili 2007). Other techniques include the quartz crystal microbalance (QCM; Krim & Widom 1988) and scanning probe

* Author for correspondence (jah@usna.edu).

One contribution of 8 to a Theme Issue 'Nanotribology, nanomechanics and applications to nanotechnology I'.

microscopies (Binnig *et al.* 1986; Carpick & Salmeron 1997; Gnecco *et al.* 2007). While all these techniques have played pivotal roles in the examination of the fundamental origins of friction, the atomic force microscope (AFM) is, perhaps, the most widely used technique. The AFM is used to investigate the forces present, as a small tip is moved across a surface. Even with careful calibration, AFM experiments do not provide a complete picture of the individual forces between a given tip and surface atom. As computational techniques, e.g. molecular dynamics (MD), provide information about each atom present at a sliding interface, they are uniquely suited to complement experimental techniques.

2. Molecular dynamics

In contrast to quantum dynamics, classical MD deals with approximate interatomic forces. The basic set-up of MD algorithms is straightforward and has been discussed in a number of reviews (Harrison *et al.* 1999; Robbins & Müser 2001; Heo *et al.* 2005). In this technique, atoms are treated as discrete particles. The force on each atom is calculated after determining the system geometry, the positions and velocities of each atom and the boundary conditions. Atomic forces can be calculated by taking the derivative of an analytic interatomic potential energy function with respect to position or by using quantum mechanical methods (Car & Parrinello 1985). Analytic potential energy functions in classical MD simulations have proven to be very useful in simulating a wide range of phenomena. The choice of the potential energy function is critical to any simulation. The ideal potential energy function would have a simple form so that it would not be computationally intensive while capturing the essential physics and chemistry of the process of interest. The focus of this paper is classical MD simulations which make use of these potentials; however, quantum MD is briefly discussed.

3. Static versus kinetic friction

The force that is required to maintain a sliding velocity v over a certain distance d is the kinetic friction. The sliding velocity plays a major role in the kinetic friction. For the sliding of two contacts at low velocities, with a small layer of fluid confined in between the layers, the kinetic friction at the microscopic scale is seen to increase linearly with the velocity (Krim *et al.* 1991; Smith *et al.* 1996; Mak & Krim 1998). This linear response of friction can be described with the following equation:

$$F = \frac{M}{\tau} v, \quad (3.1)$$

where M is the mass of the sliding object; τ is the slip time or the time required for a moving object to slow to $1/e$ of the original sliding speed (Krim & Widom 1988); and v is the sliding speed. However, as the velocity increases, the friction no longer obeys this linear relation.

As a sliding surface moves across the stationary surface, the kinetic energy of the sliding surface is transferred to the stationary surface, causing a temperature increase. This increase can alter the face of the stationary surface, affecting the

rate at which friction increases with velocity. At intermediate velocities, the kinetic friction is given by

$$F_k \approx F_k(v_{\text{ref}}) + c \left(\ln \frac{v_0}{v_{\text{ref}}} \right)^\gamma, \quad (3.2)$$

where c is a constant; v_{ref} is the reference velocity; v_0 is the sliding velocity; and γ is an exponent that is approximately 1 (Müser 2006). At high sliding velocities, the transfer of heat could become too slow to have any effect on the friction, as the sliding surface has moved past the point of heat transfer of the stationary surface. When this occurs, the friction deviates from linearity.

Static friction is the force required to initiate sliding. The existence of this force suggests that the two surfaces are interlocked into a local free energy minimum. The friction force is the lateral force required to lift the surfaces out of the local minimum. However, there is a fundamental problem with this explanation. There is no reason why the peaks and troughs in surface free energy between surfaces should be correlated (except in the exceedingly rare case of lattice commensurability). One expects that at any moment of time, some peaks are moving up a ramp while others are moving down. The net lateral force averages to zero and there should be no static friction. Analytic and simulation studies of clean crystalline and disordered structures have supported this argument. However, macro-scaled objects almost always exhibit a finite static friction. Simulations have shown that the prevalence of static friction can be explained by third bodies, like hydrocarbons, which absorb on any surface exposed to ambient air and lock the surfaces together (He *et al.* 1999). Static friction was determined by either ramping or stepping the force until the system began to slide. A commensurate and a number of incommensurate surfaces with adsorbates were examined. In all the simulations, a finite value of static friction was observed. Every incommensurate system had approximately the same static friction with respect to a given normal load, independent of sliding direction. This indicated that the friction force is independent of surface orientation. Only the commensurate case produced different results with higher static friction, as expected, due to the uniform registry between the two surfaces.

4. Friction of crystalline surfaces

(a) Friction of diamond

The properties of diamond, such as excellent thermal conductivity, corrosion and wear resistance, and surface stability, have generated tremendous scientific and technological interest. The advent of chemical vapour deposition has sparked interest in diamond as a thin film coating for flat-panel displays, cutting tools, bearings and for micro- and nanoelectromechanical systems. Its hardness and resistance to wear makes it particularly attractive for tribological applications. As a result, it has become important to understand the friction and wear properties of diamond and diamond coatings.

Complex processes at sliding interfaces, such as roughness, grain size, surface orientation and chemical composition, can play a role in determining the surface friction. Historically, it has been proven difficult to separate the effects on friction

due to individual experimental variables using traditional macroscopic tribological experiments. In contrast, modern nanoscale AFM measurements and MD simulations provide an opportunity to vary individual parameters, such as load, contact pressure, sliding direction, sliding speed and environment, to gain insight into the fundamental friction mechanisms of diamond.

Energy dissipation in diamond systems was examined using MD (Harrison *et al.* 1995; Perry & Harrison 1995). When two diamond surfaces were in sliding contact, opposing atoms interact. The friction force varied with the periodicity of the atomic lattice and the maxima corresponded to points of strong interaction (mechanical deformation) between hydrogen atoms on opposing surfaces. The vibrational excitation (heating) of the surface bonds generated by this interaction is the essence of wearless friction. In general, this excitation increased with increasing load, causing an increase in atomic-scale friction. Several ways to alter the vibrational excitation of the interface during sliding were identified. These include replacing a few hydrogen atoms on the surface of the diamond with chemically bound methyl, ethyl and *n*-propyl groups (Harrison *et al.* 1993) or placing third body molecules, such as methane, ethane etc., in between the surfaces (Perry & Harrison 1997) in sliding contact. In general, the trapped third body molecules reduced friction to a greater extent than chemically bound groups. The trapped molecules acted as a boundary layer lubricant keeping the sliding surfaces apart and thereby reducing the vibrational excitation. The smallest molecule examined, methane, produced the largest reduction in friction because its small size and flexibility made it easier to avoid the strong collisions with the surface molecules during sliding. In contrast, chemically attaching groups to diamond reduced their ability to avoid strong collisions with the surface. In that case, the larger attached groups reduced friction more due to the increased flexibility that comes with increasing the length of the carbon atom chain.

There are several ways in which the conditions of these early simulations were not well-matched to nanoscale experiments. For example, both contacting surfaces were infinitely flat. Thus, the application of load caused the uniform compression of both materials over a constant contact area, rather than non-uniform compression of the materials and a varying contact area with load that occurs with a curved surface. Recently, a joint MD-AFM study of diamond(001)(2×1)-H and diamond(111)(1×1)-H was undertaken where the conditions were designed to correspond as closely as possible (Gao *et al.* 2007). Wearless friction as a function of load, surface orientation and sliding direction on individual crystalline grains of diamond was examined. The simulations used the second-generation reactive empirical bond-order (REBO) potential, which reproduces the zero Kelvin elastic constants of diamond (Brenner *et al.* 2002). As the extraction of shear strengths from AFM data using continuum theory requires knowledge of the mechanical properties of the tip and the sample, the accurate modelling of the elastic properties is central to the correspondence between the simulation and the experiment.

The AFM measurements showed higher adhesion and friction forces for (001) versus (111) surfaces. However, the increased friction forces were entirely attributed to increased contact area induced by higher adhesion. No difference in the intrinsic resistance to friction, i.e. in the interfacial shear strength, was observed. The MD results showed no significant difference in friction between the

two diamond surfaces, except for the specific case of sliding at high pressures along the dimer row direction ($[\bar{1}10]$) on the (001) surface (i.e. perpendicular to the dimer C–C bond). Both the AFM and MD results showed that nanoscale tribological behaviour deviates dramatically from the established macroscopic behaviour of diamond, which is highly dependent on orientation. While the tip sizes, contact pressures, sliding speeds and precise atomic structures of the tips used in the MD simulations and the AFM experiments were different, the results were, nonetheless, essentially in agreement.

The MD simulations predicted that sliding perpendicular to the C–C dimer bonds on diamond(001) (along the $[\bar{1}10]$ direction) yields lower *average* friction at high loads than when sliding parallel to the bonds (along the $[110]$ direction) under certain conditions. Changing the tip geometry from curved to flat exacerbated this difference. This study demonstrated that the tip shape, and perhaps size, can mask or enhance this friction difference. (Reducing the size of the AFM tip also reduced the interfacial shear strength in this direction; however, it was not statistically different in any direction.) The larger spacing between the surface hydrogen atoms perpendicular to the dimer bond, and the different orientation of the carbon-hydrogen bond, allows the surface hydrogen atoms more freedom, depending upon the contact geometry of the tip, and thus friction can be lower when sliding in this direction. A second contribution could be due to the overall increased corrugation of the surface potential along the dimer bond, due to the dimer rows and the troughs between them, which increases the potential barrier that must be overcome to initiate sliding, and increases the probability of stick–slip energy dissipation.

(b) Simple models, stick–slip and superlubricity

Atomic-scale stick–slip has been observed experimentally, in simulations, and is predicted by simple friction models. The first experimental observation of atomic-scale stick–slip was obtained by Mate *et al.* (1987) using an AFM with a tungsten tip in sliding contact with the basal plane of graphite. Subsequently, many observations of atomic-scale stick–slip have been made on a variety of substrates (e.g. Carpick & Salmeron 1997; Gnecco *et al.* 2007) including diamond (Germann *et al.* 1993). Insight into the atomic-scale stick–slip phenomenon has been provided by MD simulations of two contacting diamond surfaces (Harrison *et al.* 1992*a*, 1995), of a tip and a Si surface (Landman *et al.* 1989), metal surfaces (Sorensen *et al.* 1996) and two infinite surfaces of organic monolayers in sliding contact (Glosli & McClelland 1993; Mikulski & Harrison 2001*a,b*; Chandross *et al.* 2004; Harrison *et al.* 2004; Mikulski *et al.* 2005*a,b*).

Various simple models of friction have also been used to explain ‘wearless friction’ and atomic-scale stick–slip (Tomlinson 1929; Frenkel & Kontorova 1938; Braun & Naumovets 2006). In the Tomlinson model, two atomically flat solids, A and B, are in sliding contact. The B solid has surface atoms (denoted as B_0) attached to it by harmonic springs, which can lose energy to the support through vibration. As the surfaces slide, any given B_0 atom experiences the potential, V_{AB} , arising from the interaction of the two surfaces. It is the shape of V_{AB} that ultimately governs the friction process. For strongly interacting surfaces, V_{AB} will contain various local extrema. A given B_0 atom passes through various metastable local minima upon sliding and may become ‘stuck’. Falling

from these metastable minima to a lower minimum causes B_0 to become vibrationally excited. This process is the ‘slip’ and has also been termed ‘plucking’. The vibrational energy is then dissipated to the solid as heat. Therefore, plucking results in the strain energy of translation being converted to vibrational energy, which is the essence of the atomic-scale friction process. For very weakly interacting solids, the friction vanishes since V_{AB} would contain no metastable local minima.

Computer simulations can shed additional insight into the earlier models of wearless friction. For example, the directional dependence of friction is implicit to the simple models of friction because a different placement of atoms implies a different interaction potential governing the friction process. Different atom placements are encountered when sliding in the $[1\bar{1}0]$ direction of a diamond(111)(1×1)-H surface versus the $[11\bar{2}]$ direction. Therefore, simple models would predict that the friction should be different in these two directions. In contrast, simulations and experiments indicate that other factors, such as contact area and surface alignment, must also be considered. In contrast to the predictions of the simple models, AFM measurements of the wearless friction of diamond(111)(1×1)-H and (001)(2×1)-H show no inherent friction differences as a function of sliding direction (Gao *et al.* 2007). When MD simulation conditions are designed to closely correlate with experimental conditions (finite-sized tips and the sampling of multiple configurations), the friction of diamond(111) and (001) is independent of sliding direction except for the one case mentioned earlier. However, when two infinitely flat surfaces are in sliding contact and multiple configurations are not sampled simulations, the friction of diamond(111) is anisotropic, which is consistent with the simple models of wearless friction (Harrison *et al.* 1992*a*). This geometry would be similar to an AFM single-line scan with a very small tip (or with a flake attached), where commensurate contact could be achieved. These results suggest that results obtained with smaller AFM tips may more closely match predictions from simple models.

For crystalline surfaces, it is clear that atomic-scale stick–slip also depends on the load. Microscopic measurements of friction in ultra high vacuum (UHV) between a Si tip in contact with NaCl(100) provide the experimental confirmation that when the load is reduced, and the surface interaction potential changes sufficiently, a transition from stick–slip to smooth sliding occurs (Socoliuc *et al.* 2004). When the two surfaces are commensurate and the load is appreciable, stick–slip can result. When two incommensurate surfaces are in sliding contact, superlubricity or a state of extraordinarily low friction can occur. Hirano & Shinjo (1990) were the first to suggest that the interaction potential between two surfaces, V_{AB} , could be reduced by making the surfaces incommensurate. Subsequent experiments examined the friction between muscovite mica sheets as a function of lattice misfit angle revealed that the friction was anisotropic and displayed periodicity consistent with the hexagonal symmetry of mica (Hirano *et al.* 1991).

Several accounts of the experimental observation of superlubricity have appeared in the literature. Martin *et al.* (1993) examined MoS₂ in UHV and found ultralow friction coefficients (approx. 10^{-3}). Scanning tunnelling microscopy measurements in UHV (Hirano *et al.* 1997) of a W(011) wire in contact with Si(001) showed that the friction is below the detection limit for incommensurate contacts. Recently, Dienwiebel *et al.* (2004) used a novel friction

force microscope, which allows for quantitative measurement of the friction force in three directions, to examine friction between a tungsten tip and graphite. This work clearly demonstrated that the peaks in the friction occurred at 0° and 60° scanning angles and vanished for all other angles. This result is consistent with the simple models of wearless friction described above. *Mate et al.* (1987) had speculated that the atomic-scale periodicity apparent in their friction scans was caused by a graphite flake that had adhered to the tip of the AFM, thus creating a graphite–graphite sliding interface. Despite a post-friction experiment transmission electron microscopy (TEM) analysis of the tip by *Dienwiebel et al.* (2004, 2005), no evidence of the flake was obtained. Recent *in situ* TEM analysis of a tungsten tip sliding against graphite has demonstrated the existence of a graphite flake on the tip during sliding (*Merkle & Marks* 2007). For a more complete discussion on the friction between commensurate and incommensurate contacts, the reader is referred to *Müser* (2006) and *Müser & Robbins* (2000).

In commensurate contacts, the interfacial energy is a periodic function of sliding distance because the relative alignment of atoms in each surface changes in phase as the surfaces slide past each other. Incommensurate contacts can be achieved in identical materials with different crystallographic orientations or in different materials with different lattice constants. In this case, the interfacial potential samples all the relative positions of all the surface atoms. Energy is independent of sliding distance and there is no static friction. The ‘cobblestone’ model (*Homola et al.* 1990) offers a simple explanation for this behaviour. As a cart wheel (or atom) rolls across a cobble stone street, energy is dissipated as the wheel rolls down rapidly down from the top of the cobblestone (or a peak in the surface potential) into the cracks between the cobbles and is stopped by the next cobble (or next peak in the surface potential). In the case of the commensurate lattice, all the wheels (or atoms) of the cart fall into the cracks at the same time and a significant amount of the cart’s potential energy is dissipated. In the incommensurate case, only one wheel (or atom) falls into the crack at a time and only a fraction of the potential energy is dissipated. This potential corrugation can pin two surfaces together and prevent motion. *Müser & Robbins* (2000) modelled pinning between commensurate and incommensurate surfaces using MD. Two surfaces were brought together and the top surface was allowed to diffuse over the bottom surface. Commensurate surfaces were always pinned by a periodic potential when the total surface potential grew with increased system size. However, relatively large systems may be unpinned if the surface potential is small enough. Incommensurate surfaces were completely unpinned unless they have very high elastic compliance.

Experiments of carbon nanotube rolling and sliding on graphite have shown that nanotubes have preferred orientations on graphite substrates (*Falvo et al.* 1999). These experiments showed that nanotubes preferred to roll when in-registry and slide while out-of-registry. Resisting forces measured while the nanotubes were sliding were significantly lower than those measured during rolling. Simulations of a carbon nanotube on graphite surfaces by *Schall & Brenner* (2000) showed that the difference in observed friction arises from the corrugation of the potential energy surface that the nanotube encounters as it moves across the graphite. When in-registry, the lattices of the graphite and nanotube are aligned commensurately so that the surface energy is deeply corrugated. For the nanotube to move, it must either climb out of this deep

potential well or roll. When out-of-registry, the potential corrugation is minimized and the nanotube easily slides along the substrate with very little resistance. This same effect has been used to explain the lubricating properties of graphite (Dienwiebel *et al.* 2004, 2005).

5. Tribochemistry

Placing two solid bodies in sliding contact can result in wear, often with the formation of debris. The nascent particles that form the debris can interact further, either physically or chemically, with the solid bodies or other nascent particles. This interaction of chemistry and friction is known as tribochemistry, the results of which are well known in everyday life—combustion engines break down, cutting tools become dull and bearings fail. Despite the obvious importance of these consequences, and the long history of the field of tribology, a full understanding of the atomic-scale mechanisms responsible for friction-induced wear remains elusive.

Historically, characterization of reactions that occur during sliding has proven difficult due to the fact that the sliding interfaces are typically buried and traditional analysis methods were restricted to examination of the contact region subsequent to sliding. The resurgence of the field of tribology has spurred the development of experimental methods to examine the chemistry that occurs at an interface during sliding. For example, an *in situ* analysis of the tribochemistry between diamond-like carbon (DLC) surfaces was carried out by Olsen *et al.* (1996) using internal reflection spectroscopy. This apparatus allowed for the characterization of intermediates and products formed during sliding. Scharf & Singer (2002) used *in situ* Raman spectroscopy coupled to a tribometer to examine the role of third bodies in the friction behaviour of diamond-like carbon. While examining the interface during sliding is preferable, it is not always possible. New techniques are being employed to perform careful post-mortem analysis of the sliding region. For instance, Carpick and co-workers have used X-ray photo-emission electron microscopy to examine inside and outside the wear track of ultrananocrystalline diamond. Erdemir & Eryilmaz (2007) have used time-of-flight secondary ion mass spectroscopy to obtain two- and three-dimensional maps of the wear track of DLC films. These maps provide evidence of hydrocarbon fragments within the wear tracks of highly hydrogenated DLC films. While monitoring reactants, the formation of intermediates and product formation has proven to be an experimental challenge, MD simulations are uniquely suited to this task.

(a) Chemical reactions between diamond surfaces

The study of tribochemistry using classical MD simulations requires the use of a potential energy function that is capable of modelling chemical reactions or the use of quantum methods (Koskulinna *et al.* 2005; Mosey *et al.* 2005; Koyama *et al.* 2006) to calculate the forces. The bond-order potentials (Brenner 1990; Stuart *et al.* 2000) are able to model chemical reactions in covalent materials and are thus suited to model tribochemistry.

A glimpse into the rich, non-equilibrium tribochemistry that occurs when two diamond surfaces are in sliding contact was reported by Harrison & Brenner (1994). In one set of simulations, two diamond(111)(1×1)-H surfaces were in

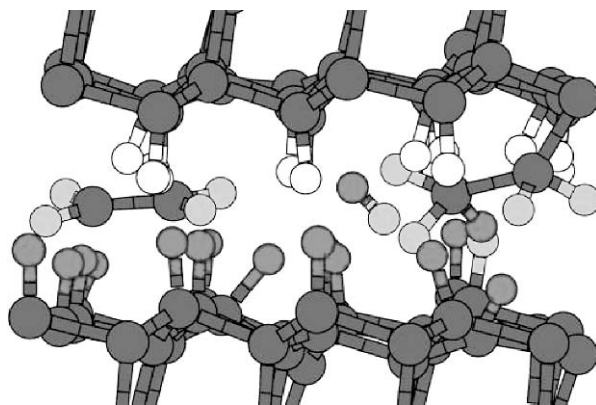


Figure 1. Close-up of the interface region between two diamond(111)(1×1)-H surfaces in sliding contact. The upper surface began the simulation with two H atoms replaced by ethyl groups. A hydrocarbon debris molecule and an H₂ molecule are the tribochemical products at the end of the simulation. Adapted with permission from Harrison & Brenner (1994).

sliding contact. In the second set, two hydrogen atoms of the upper surface were replaced with ethyl groups (–CH₂CH₃). When both surfaces were only hydrogen terminated, no chemical reactions were observed at any load or in either sliding direction examined. Chemically attaching the ethyl groups to the upper surface and repeating the sliding simulations under moderate loads (33 GPa) resulted in chemical reactions when sliding in both directions. In the [11 $\bar{2}$] direction, a complex series of chemical reactions was typically initiated by the shearing of a hydrogen atom from the tail of one of the ethyl groups. This free hydrogen atom reacted at the interface in a number of ways. One of the observed reaction sequences involved the free hydrogen atom abstracting a hydrogen atom from the lower diamond surface to form H₂. The unsaturated sites on the tail of the ethyl group and on the lower surface were then free to react, forming a covalent bond between the two surfaces. When the shear stress from sliding became too great, the adhesive bond was broken and an ethylene debris molecule was formed (figure 1). This type of debris is consistent with the type of wear debris observed in experimental studies of the macroscopic wear of diamond. The observations of these simulations are particularly important in view of the fact that they are consistent with conclusions inferred, but not directly measured, from the experimental studies of the macroscopic friction and wear of diamond.

Harrison *et al.* (1993) also examined the friction of diamond(111) surfaces with chemically bound methyl groups (–CH₃) on only one of the surfaces as a function of load and sliding direction. No tribochemical reactions were observed at any of the loads examined. Recently, quantum chemical Hartree–Fock and B3LYP methods were used to examine lateral sliding in a similar system (Koskilinna *et al.* 2005). In that work, two methyl groups were attached to opposing model diamond(111) surfaces (i.e. C₁₄H₂₄ and C₂₃H₃₆ clusters). The relative energy as a function of lateral displacement of the surfaces was monitored at a fixed interplanar distance. During lateral movement, the carbon–carbon bond that attaches the methyl groups to the model lattices was broken and the methyl group escaped from its position between the clusters. These

reactions were the result of the direct interaction of the methyl groups on opposing model surfaces. While no tribochemical reactions were observed in the MD simulations, the simulation geometry differed slightly from the quantum simulations. When the simulation systems are similar, the quantum simulations and the classical MD simulations have been shown to be in good agreement. This was demonstrated in the case of two diamond(111)(1×1)-H surfaces in sliding contact studied by both quantum (Neitola & Pakkanen 2001) and classical methods (Harrison *et al.* 1992*a*).

(*b*) *Shear-induced polymerization*

As self-assembly is a viable means of controlling the physical and chemical properties of solid surfaces, many studies have been devoted to the development of thin films of functionalized molecules for optical, electronic, mechanical or biochemical applications (Ulman 1996). Technological applications, such as microelectromechanical systems (Mastrangelo 1998) and magnetic storage devices (Karis 2002), have piqued interest in the potential use of organic films for boundary-layer lubricants. Monolayers formed from self-assembly, such as alkanethiols and alkylsilanes, which are covalently bonded to the substrate, may be good candidates for boundary-layer lubricants. As a result, the mechanical and tribological properties of self-assembled monolayer (SAM) materials have been studied a great deal using scanning probe microscopies (Carpick & Salmeron 1997; Liley *et al.* 1998; Harrison *et al.* 2004 and references therein; Li *et al.* 2005; Braun & Naumovets 2006; Brukman *et al.* 2006).

The properties of SAMs containing chains with diacetylene moieties have been studied using the AFM (Mowery *et al.* 1999; Cheadle *et al.* 2001). Because the cross-linked backbone (which is the result of exposure to UV radiation) demonstrates a chromatic response to elevated temperature and stress, these structures have the potential to be used as molecular sensors (Enkelmann 1984; Burns *et al.* 2001). The atomic-scale friction of unpolymerized diacetylene and polymerized monolayers has been examined using an AFM (Carpick *et al.* 1999; Mowery *et al.* 1999).

Chateauneuf *et al.* (2004) used MD simulations to examine the compression and friction of model SAMs composed of chains containing the diacetylene moiety. Because the AIREBO potential was used, cross-linking (polymerization) of the chains during the simulation was possible (Stuart *et al.* 2000). An irregular amorphous carbon counterface was brought into contact with three different monolayers. The location of the diacetylene moieties within the chains was varied and the effects on polymerization and friction were examined. The simulations showed that cross-linking between chains was initiated by the mechanical deformation of the monolayers. The amount of polymerization and its pattern depended upon the deformation, i.e. compression or shear and the location of the diacetylene moieties within the chains. When the diacetylene moieties were located in the middle of the chains, compression with the counter surface led to polymerization between monolayer chains only. When these moieties were on the ends of the chains, chemical reactions with the counterface also occurred. Altering the placement of the diacetylene moieties by one carbon atom within the chain, i.e. the spacer length, led to different polymerization patterns within the monolayers.

(c) Amorphous carbon films

Amorphous carbon and DLC films have a rich variety of structures and frictional properties that depend upon the deposition method used to create them. For instance, the friction of most DLC films increases sharply with time in inert environments while some DLC films exhibit super low friction when tested under similar conditions (Erdemir & Donnet 2001; Fontaine & Donnet 2007).

The tribology between a diamond(111)(1×1)-H surface and an a-C film was examined using classical MD simulations (Gao *et al.* 2002, 2003; Schall *et al.* 2007) and the REBO potential (Brenner *et al.* 2002). The effects of film thickness and sp²-to-sp³ ratio were examined. A detailed analysis of one of the sliding simulations (thin film system) showed that the simulated friction increased at the start of the simulation, oscillated about some average value, underwent a transition to lower friction and finally oscillated about a lower average friction value for the remainder of the simulation (figure 2). This behaviour is reminiscent of the experimentally observed phenomenon of ‘run-in’. An analysis of the thin film structure during sliding revealed that the initiation of sliding caused alignment of the carbon-carbon bonds within the film in the sliding direction. Continued sliding and interaction with the atoms on the counterface caused oscillations in the number of carbon-carbon bonds oriented in the sliding direction. These oscillations have the same period as the friction which corresponded to the distance between hydrogen atoms on the counterface. Sliding also caused bonds to be broken and formed within the film (intra-film reactions) and between the film and the counterface (inter-film reactions). When the inter- and intra-film reactions ceased, the average friction was reduced. In other words, the film underwent restructuring to a lower friction state. In this study, inter-film reactions in the thin film system were initiated by the shearing of a hydrogen atom from the counterface above a critical load. Inter-film reactions can be initiated at lower loads by providing unsaturated atoms for reaction. Chemical reactions between the film and the counterface increase friction by increasing adhesion between the film and the counterface. This can be achieved by systematically removing hydrogen atoms from the diamond counterface or reducing the surface passivation (Gao *et al.* 2002).

The friction between two DLC surfaces has been examined using MD. In that work, a H-terminated DLC counterface, composed mostly of sp³-hybridized carbon, was placed in sliding contact with three DLC films (an analysis of film structure is given in Schall *et al.* (2007)). Three DLC films were investigated; a hydrogen-free film (P00), a film containing 20% hydrogen (P20) and a film containing 38% hydrogen (P38). The key aspect of these films is that hydrogen was uniformly distributed inside the films. This is in marked contrast to films with hydrogen-surface passivation. These three films had relatively low sp³ : sp² ratios but showed no indication of graphite-like layering. The DLC counterface was brought into sliding contact with each of the three films and the friction as a function of load was calculated (figure 3a). The friction versus load data clearly show that passivating the amorphous carbon films with hydrogen reduces friction. The friction of the hydrogen-free (P00) film is higher than the hydrogen-containing films due to covalent bond formation (adhesion) between the

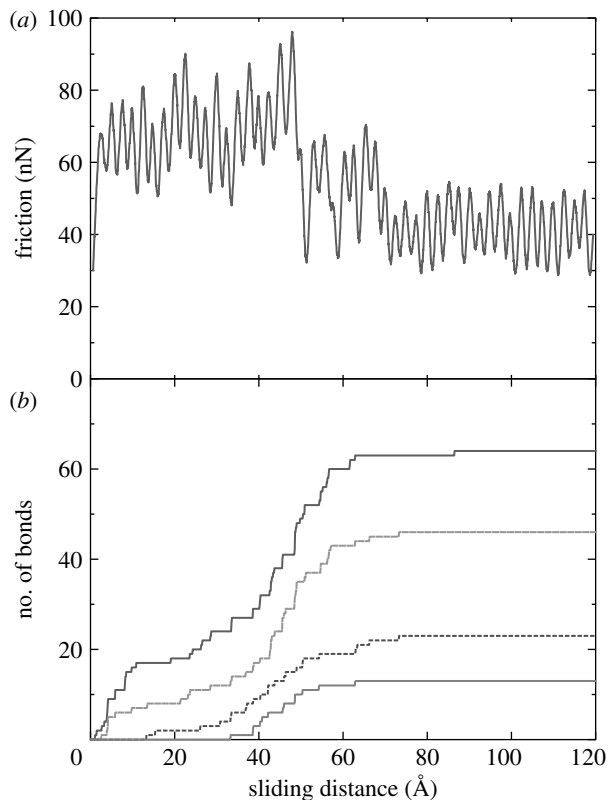


Figure 2. (a) The friction and (b) tribochemical reactions as a function of sliding distance for the thin film system (Gao *et al.* 2002). In (b), the top two lines represent intra-film bonds that are formed (top) and broken (second from top), respectively. The bottom two lines represent inter-film bonds that are formed (third line) and broken (fourth line), respectively.

counterface and the film. As in the case of two H-terminated diamond surfaces, when two DLC surfaces are in sliding contact, peaks in the friction are correlated with increases in vibrational excitation of the bonds within the film, which manifests itself as an increase in temperature. This is apparent in the plots of friction and temperature as a function of sliding distance shown in figure 3*b*. The maxima in the friction are immediately followed by an increase in the film's temperature. The region of the film closest to the interface experiences the largest increase in temperature. Closer examination of this film reveals that there is one point that is rougher (higher) than the rest of the film. It is the interaction of this area with the counter surface that is responsible for the spikes in the friction force. Thus, the periodicity in the friction force is that of the roughness of the counterface and not associated with any crystallographic spacing.

Simulations of friction between two DLC surfaces, as well as the early simulations of diamond(111)(1×1)-H against DLC illustrate the importance of surface passivation. High friction in DLC films arose from chemical bond formation between the surface and counterface due to a lack of passivation. In our earlier work, this was termed as the adhesive component of friction which is analogous to the adhesion that occurs when two diamond surfaces are brought into contact. This

adhesion has been studied using classical MD simulations (Harrison *et al.* 1992b) and more recently by first-principles DFT calculations (Ciraci *et al.* 2007). The classical MD studies examined the adhesion between infinite diamond(111) surfaces with varying amounts of hydrogen and between a H-terminated diamond asperity and an infinite diamond(111) surface. In both cases, the removal of hydrogen atoms caused the creation of unsaturated sites, or dangling bonds, that served as initiation points for adhesion (covalent bond formation) between the two contacting bodies. The first-principles DFT calculations between diamond(001) slabs confirmed the importance of hydrogen in passivating diamond surfaces and provided additional insight into the charge distribution for H-terminated and hydrogen-free surfaces.

(d) Quantum MD

The frictional properties of the antiwear additive zinc dialkyldithiophosphate (ZDDP) were recently examined using Car–Parrinello *ab initio* MD simulations (Mosey *et al.* 2005). The response of antiwear additives to extreme tribological conditions (large flash pressures p_{\max} and temperatures T_{\max}) was investigated by examining the response of bulk zinc phosphate to various values of p_{\max} . The simulation cells were composed of one triphosphate ($\text{P}_3\text{O}_{10}\text{H}_5$) and one or two zinc phosphate molecules ($\text{Zn}[\text{PO}_4\text{H}_2]_2$) with periodic boundary conditions imposed. This choice of starting conditions models the decomposition products of the antiwear additive ZDDP. The simulations were carried out by linearly increasing the pressure until some predetermined value of p_{\max} was reached. Once p_{\max} was reached, the pressure was decreased at the same rate. The results of all the simulations were in general agreement, irrespective of compression rate, initial alignment of molecules, temperature or system size. The application of pressure greater than approximately 6 GPa caused cross-linking of the system where the Zn sites adopted a tetrahedral geometry. An additional increase in pressure (approx. 17 GPa) produced a highly cross-linked configuration in which the Zn was hexacoordinate. This structure exhibited three-dimensional cross linking (figure 4). When the pressure was reduced below approximately 7 GPa, the Zn returned to its tetracoordinate state. The formation of the cross-linked networks increased the bulk modulus and shear modulus of the films. This is consistent with the experimental data, which show that the harder one pushes on these films the harder they become (Bec *et al.* 1999).

6. Links between friction, structure and disorder in SAMs

The frictional properties of SAMs have been studied extensively using scanning probe microscopies (Carpick & Salmeron 1997; Gnecco *et al.* 2007). The effects of chain length, packing density and terminal group on friction are some of the variables that have been examined. This experimental work has motivated a number of theoretical studies of the friction of SAMs. For a more complete review of this theoretical work, the reader is referred to Harrison *et al.* (2004).

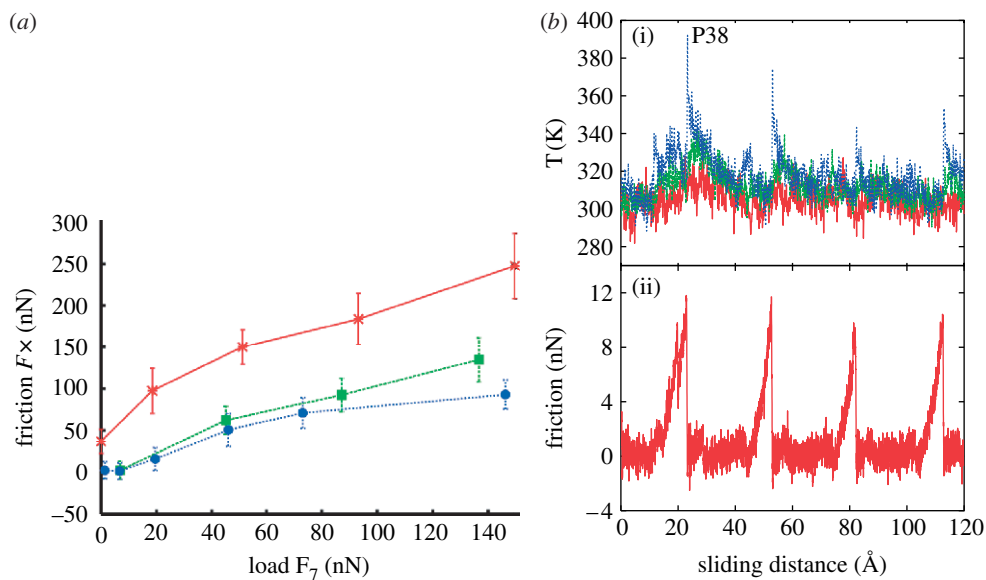


Figure 3. (a) Friction force as a function of applied load when a DLC tip is in sliding contact with a-C films with different amounts of hydrogen (red solid line, P00; green dashed line, P20; and blue dotted line, P38). (b) (i) Temperature and (ii) friction force as a function of sliding distance when a DLC tip is in sliding contact with the P38 (DLC) film. The load is held constant at 0 nN. The upper region of the surface represented by the blue line in (i) is closest to the sliding interface (red solid line, bottom; green dashed line, middle; blue dotted line, upper).

(a) SAMs with ideal packing

For alkanethiols on Au(111), multiple experiments have found the orientation of the chains to be in an all-trans conformation with a cant of 30° (Ulman 1996). This arrangement of chains serves as the ideal geometry and is the starting point for many simulations that have examined the friction of SAMs (Harrison *et al.* 2004). For example, Mikulski & Harrison (2001b) used classical MD simulations and the AIREBO potential to examine the periodicities associated with sliding a diamond(111)(1×1)-H surface across a monolayer composed of alkane chains. Chains with 13 carbon atoms were chemically bound to a diamond(111) surface in the (2×2) arrangement yielding approximately the same packing density and cant as observed in monolayers composed of alkanethiols on Au(111). It should be emphasized that these simulations correspond to an ideal case because the counterface is atomically flat and commensurate with a tightly packed, and nearly defect free, monolayer. This idealized situation gives rise to many periodic properties associated with sliding, some of which are discussed below.

In these simulations, the rigid layers of the diamond(111)(1×1)-H counterface were moved towards the monolayer at a constant velocity to apply a load. After equilibrium was established at a given load, the rigid layers were moved at a constant velocity in the sliding direction. During the course of sliding along the direction of chain cant, the following quantities were monitored: the force vector exerted by the counterface on the full monolayer of chains; the positions

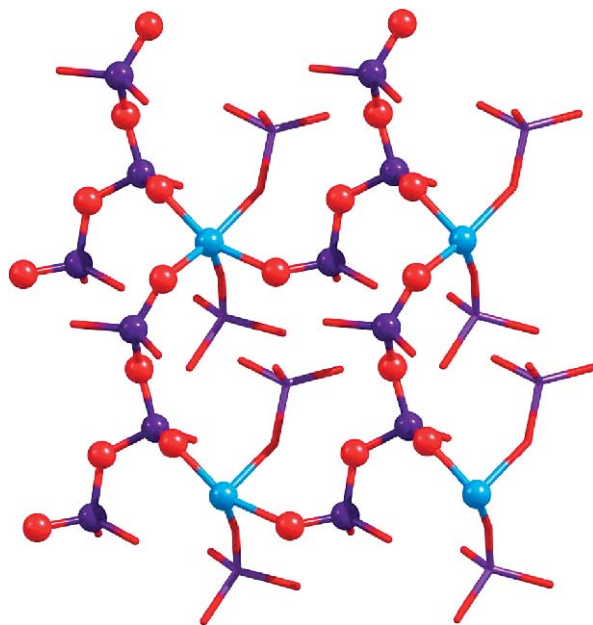


Figure 4. Representative structure of the cross-linking of the zinc phosphate system that occurs when compressed to approximately 17 GPa. The zinc atoms are hexacoordinate in all cases; however, some of the bonds corresponding to interactions between atoms in periodically repeated cells are not shown. Blue, purple and red spheres correspond to zinc, phosphorus and oxygen atoms, respectively. (Adapted with permission from Mosey *et al.* (2005).)

of the terminal carbon atoms within each chain; the change in length of the carbon backbone of each chain; the total energy of the system E (kinetic + potential + work done by bath); and the azimuthal angle ϕ , which was taken to be the average angle between the sliding direction and the projection of each carbon backbone in the plane that contains the monolayer. As the counterface slides over the monolayer, analysis of the angle ϕ showed the chains getting pushed from side to side as each wave of the hydrogen atoms of the counterface passed by. Animated sequences of the simulation revealed that all chains move to the same side in a synchronized motion. The motion is not symmetric about zero (though it does pass through zero); this shows that the chains were preferentially shifted to one side. Thus, it is only after sliding through one unit cell that the chains returned to the starting geometry. The same periodicity was observed in a number of quantities, with some examples shown in figure 5. As each wave of hydrogen atoms from the counterface interacts with the top of the chain during sliding, the chains were slightly compressed and stretched. When the counterface hydrogen atoms passed by the top of the chains, the chains sprang back to the uncompressed, unstretched state. The stretching out in the sliding direction extended throughout the entire chain. This is also known as the ‘stick’ in the atomic-scale stick–slip phenomenon. During the spring back phase, or the slip, the friction force F_y changes sign, and decreases dramatically, as the chains push the counterface hydrogen atoms (figure 5). It is important to note that the fluctuations in the friction force are significantly larger than the

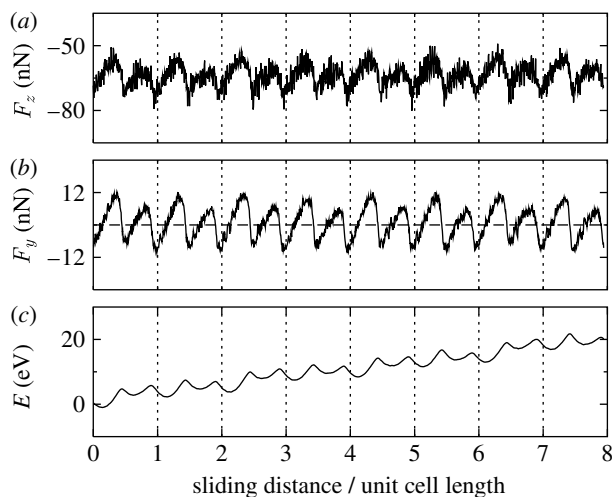


Figure 5. Average system energy E , friction F_y and normal forces F_z on the counterface as a function of sliding distance. The average load on the system is 64 nN (approx. 8 GPa). The sliding distance has been divided by the unit cell length of the (2×2) packing of the chains. Adapted from Mikulski & Harrison (2001*b*).

average force. The implication being that while the motion of the counterface on the whole is steadily depositing energy into the system (slope of E in figure 5), at any given instant it can either be depositing or removing energy to this system depending on whether it is pushing the chains or being pushed by them. This is evident in figure 5, which shows the total energy of the system E . The periodicity associated with F_y is very regular implying that the channels for energy dissipation associated with this force should exhibit this extremely regular periodic behaviour.

All the periodic quantities associated with sliding exhibited a start-up sliding effect with the final shape of the period oscillation achieved after two or three unit cells. This sort of start-up effect is also apparent in the simulations of two, well-ordered hydrocarbon monolayers on SiO_2 in sliding contact (Chandross *et al.* 2004). In the analysis of kinetic friction, data from these first few cycles should be ignored. This effect can be avoided by equilibrating the systems while sliding (Mikulski *et al.* 2005*a,b*). This method has the added advantage of allowing for some settling of the disorder caused by the randomness associated with the compression of the monolayer by an infinite surface. Anytime the counterface is commensurate with a tightly packed monolayer, periodicities in the properties associated with sliding, like stick-slip, will be apparent. Classical MD simulations of two alkylsilane monolayers in sliding motion exhibit atomic-scale stick-slip with the same periodicity as the monolayer for all the velocities examined (Chandross *et al.* 2002). The magnitude of the oscillations can be enhanced by increasing the strength of the attraction between the monolayers and the counterface. This was demonstrated nicely by Park *et al.* (2003) in their examination of the friction between opposing alkanethiol SAMs with $-\text{CH}_3$, $-\text{OH}$ and $-\text{COOH}$ terminations (figure 9).

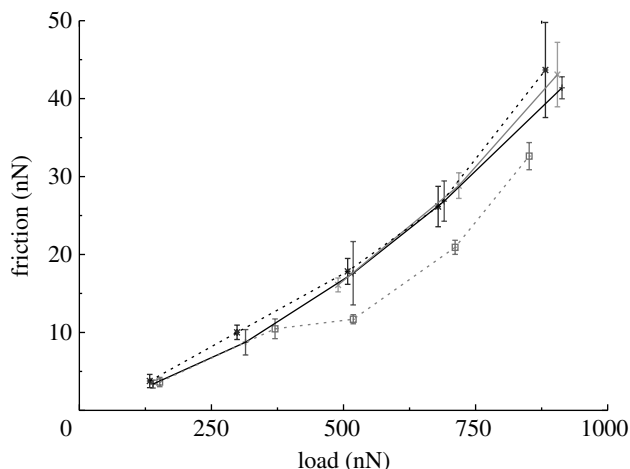


Figure 6. Friction versus load when a diamond(111)(1×1)-H surface is in sliding contact with monolayers composed of 72 C₁₈ alkane chains. Data represented by the black solid line is for chains attached to diamond(111) in the (4×4) arrangement. All other systems had the chains attached in the (2×2) arrangement. The tightly packed system (grey dashed line) has 72 chains. Twenty and forty (2×2) chains have been randomly removed from the surfaces represented by the black dashed and grey solid lines, respectively. Adapted from Mikulski & Harrison (2001a) and Harrison *et al.* (2004).

(b) Structural effects and disorder

It is important to note that the MD simulations described above used idealized geometries, which can be difficult to attain experimentally. Even in well-packed alkanethiol SAMs, with a chain-to-chain spacing of approximately 5 Å, domains and defects exist (Ulman 1996). In addition, decreasing the length of the alkane chain changes the packing density of the alkanethiol SAMs. It is also possible to make SAMs with chains of mixed lengths. Therefore, while the examination of idealized geometries using computer simulations yields important information, there is a need to examine systems which fall outside this classification. Some of the variables that have been examined are packing density (or defect density) (Mikulski & Harrison 2001a; Chandross *et al.* 2004; Harrison *et al.* 2004), mixed chain lengths (Mikulski *et al.* 2005a), the odd–even effect (Mikulski *et al.* 2005b) and surface termination (Park *et al.* 2003).

Mikulski & Harrison (2001a) examined the effects of packing density, or defect density, in SAMs by randomly removing 20 chains (approx. 30%) from a monolayer composed of C₁₈ alkane chains on diamond. The idealized monolayer, composed of 72 tightly packed chains in the (2×2) arrangement, served as the control system. The diamond(111)(1×1)-H surface was always used as the counterface. Additional defect densities and packing arrangements were also examined and friction results with double the defect density for a (4×4) packing arrangement were very similar to the data for the monolayer with approximately 30% defects (figure 6; Harrison *et al.* 2004). The creation of defects within the monolayer disrupts both the tight packing of the monolayer and the concerted response of the chains to the motion of the counterface, which leads to higher friction. As a result, the friction force as a function of sliding distance loses the

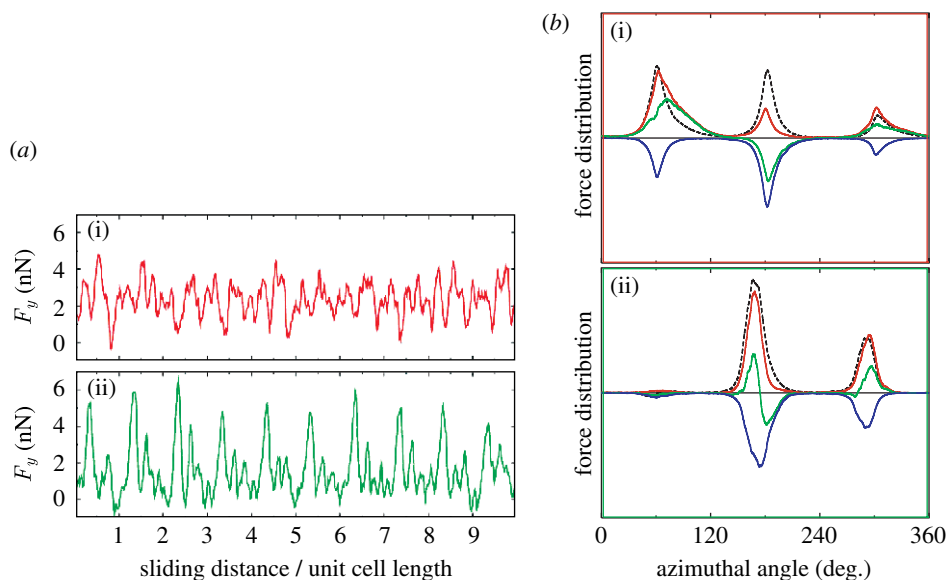


Figure 7. (a) Friction force versus sliding distance for monolayers composed of (i) C_{13} (odd) and (ii) C_{14} (even) (SAM) alkane chains. The sliding distance has been divided by the (2×2) unit cell distance of diamond. The load of 40 nN corresponds to 1.8 GPa. (b) Contact force distributions for the three terminal hydrogen atoms in each chain as a function of azimuthal angle when an amorphous carbon counterface is in sliding contact with (i) odd and (ii) even monolayers (figure 8a). Friction (green line) is the sum of the resisting (positive) and pushing (negative) contact forces (black, load; red, resist; green, net; blue, push). A detailed description of the contact forces is given in Mikulski *et al.* (2005b).

periodicity associated with the (2×2) unit cell and the average friction is higher (Mikulski & Harrison 2001a). The effect of defect density on the friction between two SAMs composed of alkane chains attached to SiO_2 was examined by Chandross *et al.* (2004) using MD and the COMPASS force field. Friction between commensurate, defect-free SAMs and SAMs with 10, 30 and 50% of the chains randomly removed was examined. The periodicity of properties like shear stress, as a function of sliding distance, was also destroyed by the creation of defects in the opposing SAMs.

Even slight disruptions within the monolayer, or breaking of the commensurability between the monolayer and the counterface, perturb the regular periodic shape of the friction force as a function of sliding distance. For example, Mikulski *et al.* (2005b) used a H-terminated, amorphous carbon counterface and MD to examine the friction model of SAMs composed of C_{13} alkane chains (referred to as the odd system) or C_{14} chains (referred to as the even system) attached to diamond(111) in the (2×2) arrangement (figure 8a). The friction response of these monolayers was examined over the load range 20–320 nN (0.9–14.4 GPa). The counterface was incommensurate with the monolayers and nominally flat to minimize roughness effects. Because the counterface is no longer commensurate with the monolayer, the friction as a function of sliding distance becomes slightly more irregular than the perfectly repeating patterns shown in figure 5. While the friction force versus time

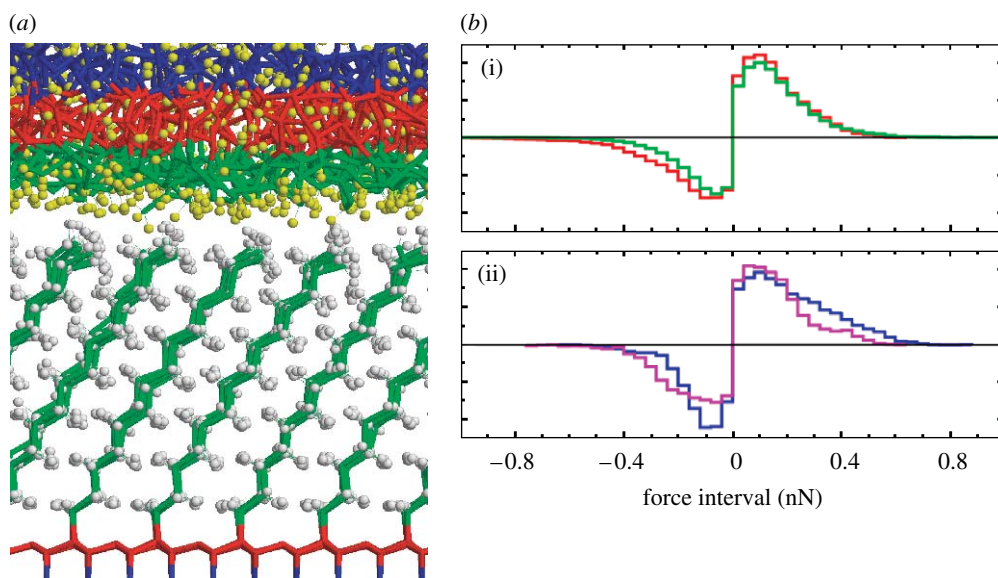


Figure 8. (a) H-terminated amorphous carbon counterface (top) in contact with a monolayer of C_{14} alkane chains attached to diamond(111) in the (2×2) arrangement. (b) Contact force distributions in the sliding direction for the top 100 $-CH_3$ and top 100 $-CH_2-$ chain groups for pure (C_{14} chains) and the top 200 groups for the mixed monolayers. The sliding direction is along the direction of chain cant and transverse to the chain cant in (i) (red, pure; green, mixed) and (ii) (blue, pre-transition; pink, post-transition), respectively. Positive forces correspond to chain groups resisting counterface motion, while negative (restoring) forces indicate groups pushing the tip along. For simulation details see Mikulski *et al.* (2005a).

for the C_{14} monolayer is periodic (figure 7a), it has more structure than when the commensurate, atomically flat diamond counterface was used. Changing the number of carbon atoms in the chains to 13, introduces slightly more disorder at the interface (Mikulski *et al.* 2005b) and, as a result, the friction versus sliding distance plot for this system at the same load is less regular than it is for the monolayer composed of C_{14} chains (figure 7a). The application of load to the odd system resulted in more structural changes at the interface than in the even system. As a result, the friction versus time at higher loads (figure 7a) of the even system is still somewhat ordered; however, these data are less ordered in the odd system.

Mikulski *et al.* (2005b) also found that the average friction of the odd system was higher than the friction of the even system at all but the lowest loads examined. The difference in friction between these two systems was ultimately attributed to structural differences in the monolayers at the sliding interface. An analysis of the contact forces on the terminal hydrogen atoms of each chain revealed interesting differences in the way load and friction forces are distributed in the even and odd systems (figure 7b). In the even system, the hydrogen atom that is protruding into the monolayer, below its parent carbon atom, has no contact forces on it. The peak at 180° corresponds to the H atom that is the highest distance above the monolayer. This H atom carries most of the load and contributes a negligible amount to the net friction. The third H atom has a larger contribution to the friction but carries only a small amount

of the load. In contrast, in the odd system, all three of the terminal hydrogen atoms had appreciable contact forces although the forces on one hydrogen were small. There was an interesting interplay between the two hydrogen atoms with the largest forces with one of these atoms predominately resisting tip motion while the other assists tip motion. Taken together, these two hydrogen atoms were responsible for most of the friction.

There are many ways to introduce disorder in a SAMs-containing system, which disrupts the periodicity of the friction versus sliding distance data and ultimately increases the friction. Perry and co-workers (Lee *et al.* 2000) used an AFM to examine the friction of SAMs composed of spiroalkanedithiols. The use of this type of molecule allows the effects on friction of crystalline order at the sliding interface to be unambiguously probed. The spiroalkanedithiol molecules attach to the substrate and then branch into two chains. Systematically shortening one of the chains caused a progressive increase in disorder and an increase in friction.

Motivated by experimental work that examined the friction of mixed chain length SAMs, Mikulski *et al.* (2005a) used MD to investigate monolayers of *n*-alkane SAMs composed of chains of a single length (pure) and those composed of chains of two lengths (mixed). As in previous studies, the chains were chemically bound to a diamond(111) substrate in the (2×2) arrangement and the amorphous hydrocarbon counterface shown in figure 8a was used to probe friction. The pure system was composed of 100 C₁₄ alkane chains and the mixed system contained equal amounts of C₁₂ and C₁₆ alkane chains. The connection between contact forces, between the counterface and the chain groups, during sliding and the structure and mobility of the monolayer chains was examined. Structural differences, or disorder, at the sliding interface caused both the friction force and the average deviation in the position of the ends of the chains in the mixed system to lose periodicity. The net friction of the mixed system was higher. The individual contact forces on the top 100 -CH₃ and -CH₂ groups within each chain were plotted as a histogram (figure 8b). The shape of the contact force distributions containing the positive forces is similar in both the pure and mixed systems. Therefore, the pure and mixed systems resist the motion of the counterface in a similar way. In contrast, the negative (forces that 'push' the tip along) contact forces of the pure and mixed systems are markedly different. This suggests that the ordered structure of the pure systems is conducive to returning the energy stored during resistive processes as mechanical energy to the monolayer, while the disordered, slightly less dense, structure of the mixed systems at the sliding interface results in the conversion of the stored potential energy into thermal energy. The resistive forces at medium to high force intervals indicate that the scale of forces is similar in the pure and mixed systems. While the larger forces in the pure systems at small positive force intervals indicate a more densely packed structure that brings more chain groups in more frequent contact with the tip. With its densely packed structure, the groups in the pure monolayer exhibit a much higher level of symmetry between positive and negative forces along the sliding direction (figure 8b). As a result, when the positive and negative forces are added, the net friction is small. The positions of chain groups in the mixed system as a function of time vary over a much wider range than the groups in the pure system. This points to a correlation between restricted range of motion and lower friction with the coordinated response of chains during sliding in the pure system aiding in the recovery of mechanical energy, which leads to low net friction.

(c) Friction anisotropy

The AFM and related force microscopies have been used to measure friction anisotropy in a number of systems, including SAMs (Carpick & Salmeron 1997; Carpick *et al.* 1999; Chen *et al.* 2006). For example, Liley *et al.* (1998) used a lateral force microscope to measure friction of a lipid monolayer in the wearless regime. The monolayer contained domains with long-range orientational order and larger friction anisotropies and non-negligible friction asymmetries were measured. MD simulations have also been used to examine the dependence of friction on sliding direction in the pure and mixed SAMs described above (Mikulski *et al.* 2005*a*). At the beginning of the slides, the cant of chain backbones is nearly perpendicular to the sliding direction. In this work, four independent starting configurations were examined for both the mixed and pure systems. Upon sliding transverse to chain cant, all four of the mixed systems underwent a transition corresponding to a rotation of 60° of the chains within the monolayer. After the transition, the cant of the reoriented chains was more closely aligned with the sliding direction. In contrast, only two of the pure systems successfully transitioned to this new chain orientation in the same sliding distance.

Both the mixed and the pure systems exhibited higher friction when sliding transverse to the chain cant, compared to sliding in the direction of chain cant. This is apparent from examination of the contact force distributions for the pure system when sliding transverse to the tilt direction (figure 8*b*). Before the collective rotation of the chains (pre-transition), the forces resisting the motion of the counterface are larger than when sliding with the chain cant. In addition, there is a significant asymmetry between the resistive and restoring (negative) forces that leads to a net friction that is a factor of two larger than it is when sliding along the chain cant. Once the chains have been realigned in the sliding direction (post-transition), the contact force distribution changes and more closely resembles the distribution of the pure system when sliding along the chain cant.

(d) Chemical effects

One interesting way to examine the chemical contributions to friction is to compare the friction of SAMs with different chemical species on the ends of the chains while using the same tip to probe the samples. The effect of fluorination on friction was examined using an AFM by comparing the response of -CH₃- and -CF₃-terminated SAMs (Kim *et al.* 1999; Houston *et al.* 2005). The effect of -OH termination (Brewer & Leggett 2004) and -COOH termination (Houston & Kim 2002) on friction has also been examined. Park *et al.* (2003) used MD to examine the friction between two monolayers of alkanethiol SAMs with -CH₃, -COOH or -OH termination. Initially the monolayers were in their ideal packing geometry. The all-atom COMPASS force field was used, which allows for partial charges that arise from electronegativity differences between atoms but does not allow for chemical reactions. Both the -CH₃ and -COOH-terminated films exhibited stick-slip (figure 9). The periodicity of the -COOH-terminated chains corresponded to the periodicity of the chains because the sticking was due to hydrogen bonding across the sliding interface. When the chains were -CH₃ terminated, the terminal C-C bond is nearly parallel to the substrate. As a result, both the terminal -CH₂- and -CH₃ groups interacted with the opposing monolayer resulting in a smaller

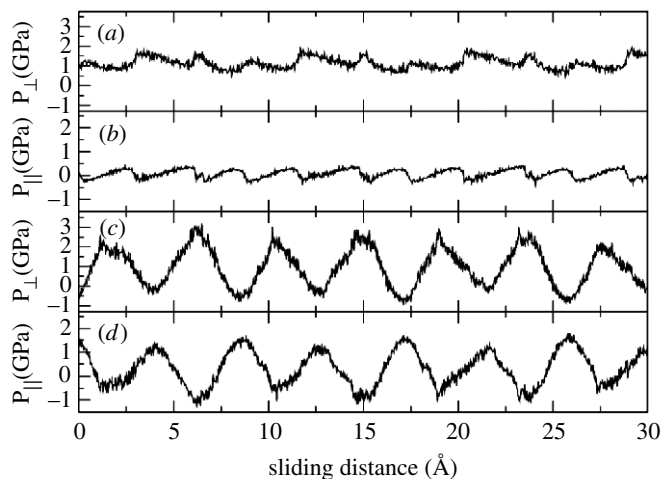


Figure 9. Friction between alkanethiol films. (a) Normal stress and (b) shear stress for $(\text{CH}_2)_8\text{CH}_3$ chains; (c) normal and (d) shear stress for $(\text{CH}_2)_8\text{COOH}$ chains. See Park *et al.* (2003) for simulation details.

periodicity than the spacing between chains. The increased adhesion between the $-\text{COOH}$ -terminated monolayers from the hydrogen bonding is responsible for the larger fluctuations in the shear stress, compared to the $-\text{CH}_3$ -terminated chains.

7. Summary and outlook

Since the positions and velocities of all atoms are known at each time step, MD simulations can provide unique atomic-scale insight into processes that occur at sliding interfaces. In this review, we have highlighted some of the insights that have shed light on the friction of SAMs, carbon-containing systems and antiwear additives. While it is true that the length and time scales of AFM experiments and MD simulations do not correspond exactly, much insight into experimental data can still be provided by MD. Increases in computational power and algorithm development (e.g. hybrid finite element and MD simulations) continue to increase the time and length scales available to simulations. At the same time, unique experimental methods to probe the interface during sliding at smaller and smaller length scales continue to be developed. Thus, the gap between experiments and simulations continues to narrow. Continued work in these areas will provide the tools that will allow for the fundamental origins of friction to be unlocked.

J.D.S., J.A.H. and G.G. acknowledge the support from AFOSR under contracts F1ATA053001G001 and F1ATA053001G004 (Extreme Friction MURI). J.A.H., M.T.K. and P.T.M. acknowledge the support from the ONR under contract N0001406WR20205. J.A.H. thanks N. Mosey and M. Chandross for providing figures from their work.

U.S. Government Employee Certification: this will certify that all authors of the work are U.S. government employees and prepared the work on a subject within the scope of their official duties. As such, the work is not subject to U.S. copyright protection.

References

- Bec, S., Tonck, A., Georges, J. M., Coy, R. C., Bell, J. C. & Roper, G. W. 1999 Relationship between mechanical properties and structures of zinc dithiophosphate anti-wear films. *Proc. R. Soc. A* **455**, 4181–4203. (doi:10.1098/rspa.1999.0497)
- Binnig, G., Quate, C. F. & Gerber, C. 1986 Atomic force microscope. *Phys. Rev. Lett.* **56**, 930–933. (doi:10.1103/PhysRevLett.56.930)
- Braun, O. M. & Naumovets, A. G. 2006 Nanotribology: microscopic mechanisms of friction. *Surf. Sci. Rep.* **60**, 79–158. (doi:10.1016/j.surfrep.2005.10.004)
- Brenner, D. W. 1990 Empirical potential for hydrocarbons for use in simulating the chemical vapor deposition of diamond films. *Phys. Rev. B* **42**, 9458–9471. (doi:10.1103/PhysRevB.42.9458)
- Brenner, D. W., Shenderova, O. A., Harrison, J. A., Stuart, S. J., Ni, B. & Sinnott, S. B. 2002 Second generation reactive empirical bond order (REBO) potential energy expression for hydrocarbons. *J. Phys. Condens. Matter* **14**, 783–802. (doi:10.1088/0953-8984/14/4/312)
- Brewer, N. J. & Leggett, G. J. 2004 Chemical force microscopy of mixed self-assembled monolayers of alkanethiols on gold: evidence for phase separation. *Langmuir* **20**, 4109–4115. (doi:10.1021/la036301e)
- Brukman, M. J., Marco, G. O., Dunbar, T. D., Boardman, L. D. & Carpick, R. W. 2006 Nanotribological properties of alkanephosphonic acid self-assembled monolayers on aluminum oxide: effects of fluorination and substrate crystallinity. *Langmuir* **22**, 3988–3998. (doi:10.1021/la052847k)
- Burns, A. R., Carpick, R. W., Sasaki, D. Y., Shelnutt, J. A. & Haddad, R. 2001 Shear-induced mechanochromism in polydiacetylene monolayers. *Tribol. Lett.* **10**, 89–96. (doi:10.1023/A:1009018110915)
- Car, R. & Parrinello, M. 1985 Unified approach for molecular-dynamics and density-functional theory. *Phys. Rev. Lett.* **55**, 2471–2474. (doi:10.1103/PhysRevLett.55.2471)
- Carpick, R. W. & Salmeron, M. 1997 Scratching the surface: fundamental investigations of tribology with atomic force microscopy. *Chem. Rev.* **97**, 1163–1194. (doi:10.1021/cr960068q)
- Carpick, R. W., Sasaki, D. Y. & Burns, A. R. 1999 Large friction anisotropy of a polydiacetylene monolayer. *Tribol. Lett.* **7**, 79–85. (doi:10.1023/A:1019113218650)
- Chandross, M., Grest, G. S. & Stevens, M. J. 2002 Molecular simulations of ordered monolayers. *Langmuir* **18**, 8392–8399. (doi:10.1021/la025598y)
- Chandross, M., Webb, E. B., Stevens, M. J., Grest, G. S. & Garofalini, S. H. 2004 Systematic study of the effect of disorder on nanotribology of self-assembled monolayers. *Phys. Rev. Lett.* **93**, 166 103. (doi:10.1103/PhysRevLett.93.166103)
- Chateauneuf, G. M., Mikulski, P. T., Gao, G. T. & Harrison, J. A. 2004 Compression- and shear-induced polymerization in model diacetylene-containing monolayers. *J. Phys. Chem. B* **108**, 16 626–16 635. (doi:10.1021/jp048077n)
- Cheadle, E. M. *et al.* 2001 Polymerization of semi-fluorinated alkane thiol self-assembled monolayers containing diacetylene units. *Langmuir* **17**, 6616–6621. (doi:10.1021/la010828e)
- Chen, J., Ratera, I., Murphy, A., Ogletree, D. F., Frechet, J. M. J. & Salmeron, M. 2006 Friction-anisotropy dependence in organic self-assembled monolayers. *Surf. Sci.* **600**, 4008–4012. (doi:10.1016/j.susc.2005.12.078)
- Ciraci, S., Yildirim, T., Dag, S. & Gulseren, O. 2007 *Ab-initio* atomic scale study of nearly frictionless surfaces. In *Superlubricity* (eds A. Erdemir & J.-M. Martin), pp. 57–77. Amsterdam, The Netherlands: Elsevier.
- Dienwiebel, M., Verhoeven, G. S., Pradeep, N., Frenken, J. W. M., Heimberg, J. A. & Zandbergen, H. W. 2004 Superlubricity of graphite. *Phys. Rev. Lett.* **92**, 126 101. (doi:10.1103/PhysRevLett.92.126101)
- Dienwiebel, M., Pradeep, N., Verhoeven, G. S., Zandbergen, H. W. & Frenken, J. W. M. 2005 Model experiments of superlubricity of graphite. *Surf. Sci.* **576**, 197–211. (doi:10.1016/j.susc.2004.12.011)
- Dowson, D. 1998 *The history of tribology*. London, UK: Professional Engineering Publishing.

- Enkelmann, V. 1984 Structural aspects of the topochemical polymerization of diacetylenes. *Adv. Polym. Sci.* **63**, 91–136.
- Erdemir, A. & Donnet, C. 2001 Tribology of diamond, diamond-like carbon, and related films. In *Modern tribology handbook*, vol. 2 (ed. B. Bhushan), pp. 871–908. Boca Raton, FL: CRC Press.
- Erdemir, A. & Eryilmaz, O. L. 2007 Superlubricity in diamondlike carbon films. In *Superlubricity* (eds A. Erdemir & J.-M. Martin), pp. 253–271. Amsterdam, The Netherlands: Elsevier.
- Falvo, M. R., Taylor, R. M., Helser, A., Chi, V., Brooks, F. P., Washburn, S. & Superfine, R. 1999 Nanometre-scale rolling and sliding of carbon nanotubes. *Nature* **397**, 236–238. (doi:10.1038/16662)
- Fontaine, J. & Donnet, C. 2007 Superlow friction of a-C:H films: tribochemical and rheological effects. In *Superlubricity* (eds A. Erdemir & J.-M. Martin), pp. 273–294. Amsterdam, The Netherlands: Elsevier.
- Frenkel, F. C. & Kontorova, T. 1938 On the theory of plastic deformation and twinning. *Zh. Eksp. Teor. Fiz.* **8**, 1380.
- Gao, G. T., Mikulski, P. T. & Harrison, J. A. 2002 Molecular-scale tribology of amorphous carbon coatings: effects of film thickness, adhesion, and long-range interactions. *J. Am. Chem. Soc.* **124**, 7202–7209. (doi:10.1021/ja0178618)
- Gao, G. T., Mikulski, P. T., Chateauneuf, G. M. & Harrison, J. A. 2003 The effects of film structure and surface hydrogen on the properties of amorphous carbon. *J. Phys. Chem. B* **107**, 11 082–11 090. (doi:10.1021/jp034544+)
- Gao, G. T., Cannara, R. J., Carpick, R. W. & Harrison, J. A. 2007 Atomic-scale friction on diamond: a comparison of different sliding directions on (001) and (111) surfaces using MD and AFM. *Langmuir* **23**, 5394–5405. (doi:10.1021/la062254p)
- Germann, G. J., Cohen, S. R., Neubauer, G., Seki, H. & Coulman, D. 1993 Atomic scale friction of a diamond tip on diamond (100) and (111) surfaces. *J. Appl. Phys.* **73**, 163–167. (doi:10.1063/1.353878)
- Gosli, J. N. & McClelland, G. M. 1993 Molecular-dynamics study of sliding friction of ordered organic monolayers. *Phys. Rev. Lett.* **70**, 1960–1963. (doi:10.1103/PhysRevLett.70.1960)
- Gnecco, E., Bennewitz, R., Pfeiffer, O., Socoliuc, O. & Meyer, E. 2007 Friction and wear on the atomic scale. In *Superlubricity* (eds A. Erdemir & J.-M. Martin), pp. 483–533. Amsterdam, The Netherlands: Elsevier.
- Harrison, J. A. & Brenner, D. W. 1994 Simulated tribology: an atomic-scale view of the wear of diamond. *J. Am. Chem. Soc.* **116**, 10 399–10 402. (doi:10.1021/ja00102a006)
- Harrison, J. A., White, C. T., Colton, R. J. & Brenner, D. W. 1992a Molecular-dynamics simulations of atomic-scale friction of diamond surfaces. *Phys. Rev. B* **45**, 9700–9708. (doi:10.1103/PhysRevB.46.9700)
- Harrison, J. A., White, C. T., Colton, R. J. & Brenner, D. W. 1992b Nanoscale investigation of indentation, adhesion and fracture of diamond (111) surfaces. *Surf. Sci.* **271**, 57–67. (doi:10.1016/0039-6028(92)90861-Y)
- Harrison, J. A., White, C. T., Colton, R. J. & Brenner, D. W. 1993 Effects of chemically bound, flexible hydrocarbon species on the frictional properties of diamond surfaces. *J. Phys. Chem.* **97**, 6573–6576. (doi:10.1021/j100127a001)
- Harrison, J. A., White, C. T., Colton, R. J. & Brenner, D. W. 1995 Investigation of the atomic-scale friction and energy dissipation in diamond using molecular dynamics. *Thin Solid Films* **260**, 205–211. (doi:10.1016/0040-6090(94)06511-X)
- Harrison, J. A., Stuart, S. J. & Brenner, D. W. 1999 Atomic-scale simulation of tribological and related phenomena. In *Handbook of micro/nano tribology* (ed. B. Bhushan), pp. 525–594, 2nd edn. Boca Raton, FL: CRC Press.
- Harrison, J. A., Gao, G. T., Harrison, R. J., Chateauneuf, G. M. & Mikulski, P. T. 2004 The friction of model self-assembled monolayers. In *Encyclopedia of nanoscience and nanotechnology* (ed. H. S. Nalwa), pp. 511–527. Los Angeles, CA: American Scientific Publishers.
- He, G., Müser, M. H. & Robbins, M. O. 1999 Absorbed layers and the origin of static friction. *Science* **284**, 1650–1652. (doi:10.1126/science.284.5420.1650)

- Heo, S. J., Sinnott, S. B., Brenner, D. W. & Harrison, J. A. 2005 Computational modeling of nanometer-scale tribology. In *Nanotribology and nanomechanics: an introduction* (ed. B. Bhushan), pp. 623–691. Heidelberg, Germany: Springer.
- Hirano, M. & Shinjo, K. 1990 Atomistic locking and friction. *Phys. Rev. B* **41**, 11 837–11 851. (doi:10.1103/PhysRevB.41.11837)
- Hirano, M., Shinjo, K., Kaneko, R. & Murata, Y. 1991 Anisotropy of frictional forces in muscovite mica. *Phys. Rev. Lett.* **67**, 2642–2645. (doi:10.1103/PhysRevLett.67.2642)
- Hirano, M., Shinjo, K., Kaneko, R. & Murata, Y. 1997 Observation of superlubricity by scanning tunneling microscopy. *Phys. Rev. Lett.* **78**, 1448–1451. (doi:10.1103/PhysRevLett.78.1448)
- Homola, A. M., Israelachvili, J. N., McGuiggan, P. M. & Gee, M. L. 1990 Fundamental experimental studies in tribology—the transition from interfacial friction of undamaged molecularly smooth surfaces to normal friction with wear. *Wear* **136**, 65–83. (doi:10.1016/0043-1648(90)90072-1)
- Houston, J. E. & Kim, H. I. 2002 Adhesion, friction, and mechanical properties of functionalized alkanethiol self-assembled monolayers. *Accounts Chem. Res.* **35**, 547–553. (doi:10.1021/ar9801144)
- Houston, J. E., Doelling, C. M., Vanderlick, T. K., Hu, Y., Scoles, G., Wenzl, I. & Lee, T. R. 2005 Comparative study of the adhesion, friction, and mechanical properties of CF₃- and CH₃-terminated alkanethiol monolayers. *Langmuir* **21**, 3926–3932. (doi:10.1021/la046901t)
- Karis, T. E. 2002 Nanotribology of thin film magnetic recording media. In *Nanotribology: critical assessment and research needs* (eds S. M. Hsu & Z. C. Ying), pp. 291–325. Norwell, MA: Kluwer Academic Publishers.
- Kim, H. I., Graupe, M., Oloba, O., Koini, T., Imaduddin, S., Lee, T. R. & Perry, S. S. 1999 Molecularly specific studies of the frictional properties of monolayer films: a systematic comparison of CF₃-, (CH₃)₂CH- and CH₃-terminated films. *Langmuir* **15**, 3179–3185. (doi:10.1021/la981497h)
- Koskilinna, J. O., Linnolahti, M. & Pakkanen, T. A. 2005 Tribochemical reactions between methylated diamond (111) surfaces: a theoretical study. *Tribol. Lett.* **20**, 157–161. (doi:10.1007/s11249-005-8308-9)
- Koyama, M., Hayakawa, J., Onodera, T., Ito, K., Tsuboi, H., Endou, A., Kubo, M., Del Carpio, C. A. & Miyamoto, A. 2006 Tribochemical reaction dynamics of phosphoric ester lubricant additive by using a hybrid tight-binding quantum chemical molecular dynamics method. *J. Phys. Chem. B* **110**, 17 507–17 511. (doi:10.1021/jp061210m)
- Krim, J. 2002 Surface science and the atomic-scale origins of friction: what once was old is new again. *Surf. Sci.* **500**, 741–758. (doi:10.1016/S0039-6028(01)01529-1)
- Krim, J. & Widom, A. 1988 Damping of a crystal oscillator by an adsorbed monolayer and its relation to interfacial viscosity. *Phys. Rev. B* **38**, 12 184–12 189. (doi:10.1103/PhysRevB.38.12184)
- Krim, J., Solina, D. H. & Chiarello, R. 1991 Nanotribology of a Kr monolayer: a quartz–crystal microbalance study of atomic-scale friction. *Phys. Rev. Lett.* **66**, 181–184. (doi:10.1103/PhysRevLett.66.181)
- Landman, U., Luedtke, W. D. & Ribarsky, M. W. 1989 Dynamics of tip–substrate interactions in atomic force microscopy. *Surf. Sci. Lett.* **210**, L117–L184. (doi:10.1016/0039-6028(89)90590-6)
- Lee, S., Shon, Y. S., Colorado, R., Guenard, R. L., Lee, T. R. & Perry, S. S. 2000 The influence of packing densities and surface order on the frictional properties of alkanethiol self-assembled monolayers (SAMs) on gold: a comparison of SAMs derived from normal and spiroalkanedithiols. *Langmuir* **16**, 2220–2224. (doi:10.1021/la9909345)
- Li, S., Cao, P., Colorado Jr, R., Yan, X., Wenzl, I., Shmakova, O. E., Graupe, M., Lee, T. R. & Perry, S. S. 2005 Local packing environment strongly influences the frictional properties of mixed CH₃- and CF₃-terminated alkanethiol SAMs on Au(111). *Langmuir* **21**, 933–936. (doi:10.1021/la0488607)
- Liley, M. *et al.* 1998 Friction anisotropy and asymmetry of a compliant monolayer induced by a small molecular tilt. *Science* **280**, 273–275. (doi:10.1126/science.280.5361.273)

- Mak, C. & Krim, J. 1998 Quartz–crystal microbalance studies of the velocity dependence of interfacial friction. *Phys. Rev. B* **58**, 5157–5159. (doi:10.1103/PhysRevB.58.5157)
- Martin, J. M., Donnet, C., Lemogne, T. & Epicier, T. 1993 Superlubricity of molybdenum-disulfide. *Phys. Rev. B* **48**, 10 583–10 586. (doi:10.1103/PhysRevB.48.10583)
- Mastrangelo, C. H. 1998 Surface force induced failures in microelectromechanical systems. In *Tribology issues and opportunities in MEMS* (ed. B. Bhushan), p. 367. Norwell, MA: Kluwer Academic Publishers.
- Mate, C. M., McClelland, G. M., Erlandsson, R. & Chiang, S. 1987 Atomic-scale friction of a tungsten tip on a graphite surface. *Phys. Rev. Lett.* **59**, 1942–1945. (doi:10.1103/PhysRevLett.59.1942)
- Merkle, A. P. & Marks, L. D. 2007 Friction in full view. *Appl. Phys. Lett.* **90**, 064 101. (doi:10.1063/1.2456192)
- Mikulski, P. T. & Harrison, J. A. 2001a Packing-density effects on the friction of *n*-alkane monolayers. *J. Am. Chem. Soc.* **123**, 6873–6881. (doi:10.1021/ja010189u)
- Mikulski, P. T. & Harrison, J. A. 2001b Periodicities in the properties associated with the friction of model self-assembled monolayers. *Tribol. Lett.* **10**, 29–38. (doi:10.1023/A:1009066026845)
- Mikulski, P. T., Gao, G., Chateaufneuf, G. M. & Harrison, J. A. 2005a Contact forces at the sliding interface: mixed versus pure model alkane monolayers. *J. Chem. Phys.* **122**, 024 701. (doi:10.1063/1.1828035)
- Mikulski, P. T., Herman, L. A. & Harrison, J. A. 2005b Odd and even model self-assembled monolayers: links between friction and structure. *Langmuir* **21**, 12 197–12 206. (doi:10.1021/la052044x)
- Mosey, N. J., Müser, M. H. & Woo, T. K. 2005 Molecular mechanisms for the functionality of lubricant additives. *Science* **307**, 1612–1615. (doi:10.1126/science.1107895)
- Mowery, M. D., Kopta, S., Ogletree, D. F., Salmeron, M. & Evans, C. E. 1999 Structural manipulation of the frictional properties of linear polymers in single molecular layers. *Langmuir* **15**, 5118–5122. (doi:10.1021/la9815998)
- Müser, M. H. 2006 Theory and simulation of friction and lubrication. *Lect. Notes Phys.* **704**, 65–104.
- Müser, M. H. & Robbins, M. O. 2000 Conditions for static friction between flat crystalline surfaces. *Phys. Rev. B* **61**, 2335–2342. (doi:10.1103/PhysRevB.61.2335)
- Neitola, R. & Pakkanen, T. A. 2001 *Ab initio* studies on the atomic-scale origin of friction between diamond (111) surfaces. *J. Phys. Chem. B* **105**, 1338–1343. (doi:10.1021/jp003025t)
- Olsen, J. E., Fischer, T. E. & Gallois, B. 1996 *In situ* analysis of the tribochemical reactions of diamond-like carbon by internal reflection spectroscopy. *Wear* **200**, 233–237. (doi:10.1016/S0043-1648(96)07295-X)
- Park, B., Chandross, M., Stevens, M. J. & Grest, G. S. 2003 Chemical effects on adhesion and friction between alkanethiol monolayers: molecular dynamics simulations. *Langmuir* **19**, 9239–9245. (doi:10.1021/la0341106)
- Perry, M. D. & Harrison, J. A. 1995 Universal aspects of the atomic-scale friction of diamond surfaces. *J. Phys. Chem.* **99**, 9960–9965. (doi:10.1021/j100024a044)
- Perry, M. D. & Harrison, J. A. 1997 Friction between diamond surfaces in the presence of small third-body molecules. *J. Phys. Chem.* **101**, 1364–1373.
- Robbins, M. O. & Müser, M. H. 2001 Computer simulations of friction, lubrication, and wear. In *Modern tribology handbook* (ed. B. Bhushan), pp. 717–765. Boca Raton, FL: CRC Press.
- Ruths, M. & Israelachvili, J. N. 2007 Surface forces and nanorheology of molecularly thin films. In *Superlubricity* (eds A. Erdemir & J.-M. Martin), pp. 389–481. Amsterdam, The Netherlands: Elsevier.
- Schall, J. D. & Brenner, D. W. 2000 Molecular dynamics simulations of carbon nanotube rolling and sliding on graphite. *Mol. Simul.* **25**, 73–79. (doi:10.1080/08927020008044113)
- Schall, J. D., Mikulski, P. T., Chateaufneuf, G. M., Gao, G. T. & Harrison, J. A. 2007 Molecular dynamics simulations of tribology. In *Superlubricity* (eds A. Erdemir & J.-M. Martin), pp. 79–100. Amsterdam, The Netherlands: Elsevier.

- Scharf, T. W. & Singer, I. L. 2002 Role of third bodies in friction behavior of diamond-like nanocomposite coatings studied by *in situ* tribometry. *Tribol. Trans.* **45**, 363–371. (doi:10.1080/10402000208982561)
- Smith, E. D., Robbins, M. O. & Cieplak, M. 1996 Friction on adsorbed monolayers. *Phys. Rev. B* **54**, 8252–8260. (doi:10.1103/PhysRevB.54.8252)
- Socoliuc, A., Bennewitz, R., Gnecco, E. & Meyer, E. 2004 Transition from stick–slip to continuous sliding in atomic friction: entering a new regime of ultralow friction. *Phys. Rev. Lett.* **92**, 134 301. (doi:10.1103/PhysRevLett.92.134301)
- Sorensen, M. R., Jacobsen, K. W. & Stoltze, P. 1996 Simulations of atomic-scale friction. *Phys. Rev. B* **53**, 2101–2113. (doi:10.1103/PhysRevB.53.2101)
- Stuart, S. J., Tutein, A. B. & Harrison, J. A. 2000 A reactive potential for hydrocarbons with intermolecular interactions. *J. Chem. Phys.* **112**, 6472–6486. (doi:10.1063/1.481208)
- Tomlinson, G. A. 1929 A molecular theory of friction. *Philos. Mag.* **7**, 905–939.
- Ulman, A. 1996 Formation and structure of self-assembled monolayers. *Chem. Rev.* **96**, 1533–1554. (doi:10.1021/cr9502357)